Quantifying the Labeling and the Levels of Plant Cell Wall Precursors Using Ion Chromatography Tandem Mass Spectrometry[1][W][OA]

Ana P. Alonso*, Rebecca J. Piasecki, Yan Wang, Russell W. LaClair, and Yair Shachar-Hill

Great Lakes Bioenergy Research Center, East Lansing, Michigan 48824 (A.P.A., R.J.P., Y.W., R.W.L., Y.S.-H.); and Department of Plant Biology, Michigan State University, East Lansing, Michigan 48824 (A.P.A., R.J.P., R.W.L., Y.S.-H.)

The biosynthesis of cell wall polymers involves enormous fluxes through central metabolism that are not fully delineated and whose regulation is poorly understood. We have established and validated a liquid chromatography tandem mass spectrometry method using multiple reaction monitoring mode to separate and quantify the levels of plant cell wall precursors. Target analytes were identified by their parent/daughter ions and retention times. The method allows the quantification of precursors at low picomole quantities with linear responses up to the nanomole quantity range. When applying the technique to Arabidopsis (*Arabidopsis thaliana*) T87 cell cultures, 16 hexose-phosphates (hexose-Ps) and nucleotide-sugars (NDP-sugars) involved in cell wall biosynthesis were separately quantified. Using hexose-P and NDP-sugar standards, we have shown that hot water extraction allows good recovery of the target metabolites (over 86%). This method is applicable to quantifying the levels of hexose-Ps and NDP-sugars in different plant tissues, such as Arabidopsis T87 cells in culture and fenugreek (*Trigonella foenum-graecum*) endosperm tissue, showing higher levels of galacto-mannan precursors in fenugreek endosperm. In Arabidopsis cells incubated with [U-$^{13}C_{Fru}$]sucrose, the method was used to track the labeling pattern in cell wall precursors. As the fragmentation of hexose-Ps and NDP-sugars results in high yields of $[PO_3]^-$ and/or $[H_2PO_4]^-$ ions, mass isotopomers can be quantified directly from the intensity of selected tandem mass spectrometry transitions. The ability to directly measure ^{13}C labeling in cell wall precursors makes possible metabolic flux analysis of cell wall biosynthesis based on dynamic labeling experiments.

Plant cell walls are the most abundant renewable resources (Pauly and Keegstra, 2008a). Much of the current biotechnological research on plant cell wall synthesis involves manipulating these biosynthetic processes to obtain higher concentrations of starches or oil, which show much promise in biofuel production, or to alter cell wall composition for easier breakdown. A detailed knowledge of these processes is essential to understanding and utilizing plant cell wall materials as well as for progress in understanding plant growth and structural development (Pauly and Keegstra, 2008b). However, research into cell wall biosynthesis has been hindered by our limited understanding of the metabolic processes that produce cell walls and particularly their regulation. Progress in this area is limited by the difficulty of differentiating among the compounds involved and of analyzing the fluxes through the biochemical network of wall biosynthesis. Many of the metabolic steps involve isomeric sugars, including hexose-Ps and nucleotide-sugars (NDP-sugars) that serve as direct precursors to plant cell wall biosynthesis. Separate quantification of these sugars has been difficult to achieve.

Much of the current research on identifying and differentiating among different metabolic pathways involves the use of chromatography and mass spectrometry (MS; Wolfender et al., 2009). It has been found that liquid chromatography (LC), when linked to a triple quadrupole mass spectrometer (tandem MS [MS/MS]), can be a powerful tool to detect and specifically quantify several classes of metabolic compounds (Allwood and Goodacre, 2010). After initial compound separation by LC, analytes are directed to a triple quadrupole mass spectrometer (MS/MS), where the initial two quadrupoles separate the compounds for detection in the third quadrupole, first by selection of particular mass-to-charge (m/z) ratios of the ionized parent compounds in the first quadrupole, then by fragmentation of the compounds in the second quadrupole (Arrivault et al., 2009). This coupling method of LC-MS/MS to identify compounds has been used with several metabolites involved in plant primary metabolism recently (Cruz et al., 2008; Arrivault et al., 2009).

[1] This work was supported by the Great Lakes Bioenergy Research Center (U.S. Department of Energy, Office of Biological and Environmental Research, Office of Science grant no. DE–FC02–07ER64494) and was supported in part by the National Science Foundation, Research Coordination Networks in Biological Sciences (grant no. 0090281).

* Corresponding author; e-mail alonsoa@msu.edu.

The author responsible for distribution of materials integral to the findings presented in this article in accordance with the policy described in the Instructions for Authors (www.plantphysiol.org) is: Ana P. Alonso (alonsoa@msu.edu).

[W] The online version of this article contains Web-only data.

[OA] Open Access articles can be viewed online without a subscription.

www.plantphysiol.org/cgi/doi/10.1104/pp.110.155713

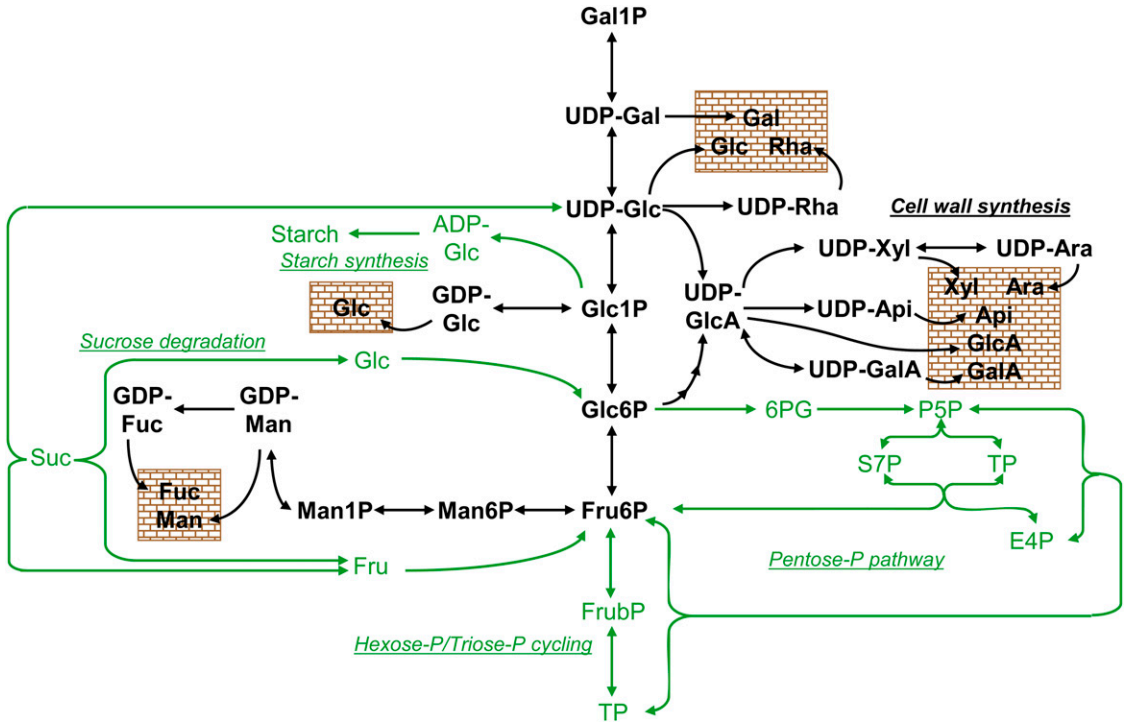

Figure 1. The metabolic network of cell wall precursors. The metabolic network of cell wall precursors is presented in black. NDP-sugars are used to build sugar residues into wall polysaccharides (brick pattern). The pathways presented in green produce or use cell wall precursors for other metabolic processes. Abbreviations not defined in text: 6PG, 6-phosphogluconic acid; bP, bisphosphate; E4P, erythrose 4-P; P5P, pentose-5-P; S7P, sedoheptulose-7-P; TP, triose-P.

Several studies have reported the separation of phosphorylated metabolites using LC-MS/MS. We are particularly interested in analyzing such compounds because plant cell wall biosynthesis involves a range of phosphorylated precursors, mainly NDP-sugars and hexose-Ps (Feingold and Barber, 1990; Fry 2000, 2004; Seifert, 2004; Somerville et al., 2004; Sharples and Fry, 2007). For example, Huck et al. (2003) and Luo et al. (2007) were able to separate, respectively, six and 28 intracellular metabolites involved in glycolysis, the oxidative pentose-P pathway, and the tricarboxylic acid cycle, some of which are phosphorylated. Bajad et al. (2006) were able to separate a large number of water-soluble cellular metabolites by hydrophilic interaction chromatography, but this method does not appear to separate isomers. Anion exchange chromatography was shown to be effective at separating phosphorylated intermediates involved in glycolysis (van Dam et al., 2002) and in the Calvin cycle (Cruz et al., 2008; Arrivault et al., 2009), especially when coupled with the high specificity and sensitivity of triple quadrupole MS. Moreover, anion-exchange chromatography coupled with MS/MS can be used to determine the mass isotopomer distribution of labeled compounds and Kiefer et al. (2007) were able to quantify isotope abundances in six phosphorylated metabolites in *Escherichia coli*.

However, some of the methods that achieved good separation of four NDP-sugars did not allow quantification by MS/MS because of the eluents used

Table I. *Specific metabolite-dependent MS parameters used in MRM*

Metabolite	[M-H]$^-$	Daughter Ion		Cone Voltage	Collision Energy
				V	*eV*
Hexose-Ps	259	97	$[H_2PO_4]^-$	25	15
UDP-Ara/UDP-Xyl	535	79	$[PO_3]^-$	34	46
UDP-Rha	549	79	$[PO_3]^-$	34	40
UDP-Glc/UDP-Gal	565	79	$[PO_3]^-$	40	40
UDP-GlcA/UDP-GalA	579	159	$[HP_2O_6]^-$	40	46
ADP-Glc/GDP-Fuc	588	159	$[HP_2O_6]^-$	46	46
GDP-Man/GDP-Glc	604	79	$[PO_3]^-$	50	40
UDP-GlcNAc/UDP-GalNAc	606	79	$[PO_3]^-$	46	46

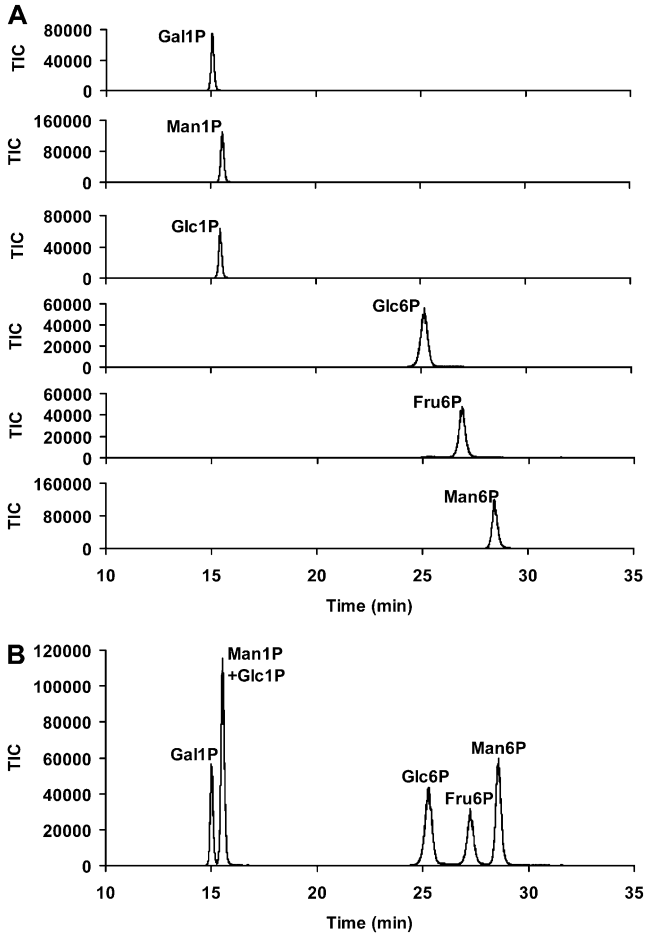

Figure 2. Analyses of hexose-P standards by LC-MS/MS. Hexose-P standards, approximately 10 μM each, were monitored by LC-MS/MS at the transition 259/97 using the separation and hardware described in "Materials and Methods." A, TIC of hexose-P standards injected individually. B, TIC of the mixture of hexose-P standards.

(Räbinä et al., 2001), and none of the methods using coupled LC-MS/MS developed to date separates all or nearly all of the hexose-Ps and NDP-sugars known to be involved in plant cell wall biosynthesis (Turnock and Ferguson, 2007). This presents a special challenge given the fact that many of these sugar compounds are diastereoisomers and ionize similarly in traditional LC-MS/MS methods. Current methods of separating hexose-Ps and NDP-sugars also involve multiple steps of chromatographic and enzymatic separation. In a notable recent study, Sharples and Fry (2007) separated many of the compounds involved in plant cell wall biosynthesis, including hexose-Ps and NDP-sugars, and used radioactive [U-^{14}C]Fru and [1-^{3}H]Gal as substrates to determine their relative contributions to different cell wall components. The method used in that study involved high-voltage paper electrophoresis separation followed by mild acid hydrolysis and/or phosphatase digestion of different fractions to release neutral hexoses that were then separated by a second paper chromatography procedure. At the cost of considerable effort, this approach allowed eight compounds to be separated. However, neither this nor many of the other approaches used to date appear to have yielded absolute metabolite levels or specific

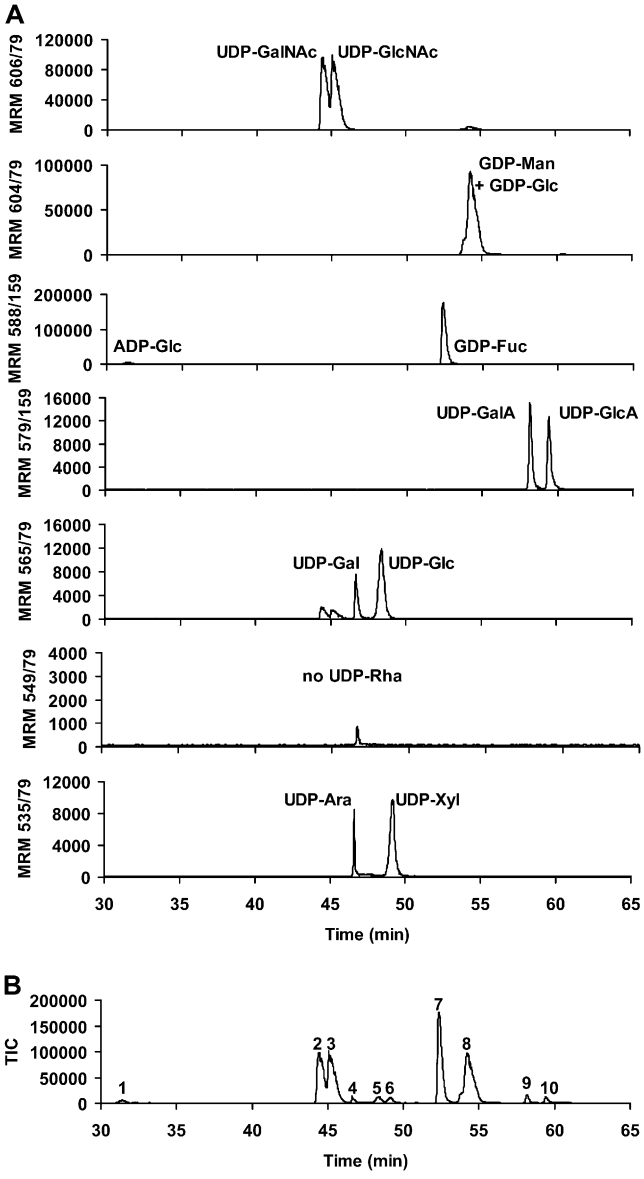

Figure 3. LC-MS/MS analyses of NDP-sugar standards. NDP-sugar standards, approximately 100 μM each with the exception of UDP-Api and UDP-Rha, which are not commercially available, were analyzed by LC-MS/MS using the separation and hardware described in "Materials and Methods." A, At different transitions; tr606/79 for UDP-GalNAc and UDP-GlcNAc, tr604/79 for GDP-Man and GDP-Glc, tr588/159 for ADP-Glc and GDP-Fuc, tr579/159 for UDP-GlcA and UDP-GalA, tr565/79 for UDP-Gal and UDP-Glc, tr549/79 for UDP-Rha, tr535/79 for UDP-Ara, UDP-Xyl, and UDP-Api. B, TIC of the mixture of NDP-sugars standards. The assigned peaks are: 1, ADP-Glc; 2, UDP-GalNAc; 3, UDP-GlcNAc; 4, UDP-Ara + UDP-Gal; 5, UDP-Glc; 6, UDP-Xyl; 7, GDP-Fuc; 8, GDP-Man + GDP-Glc; 9, UDP-GalA; 10, UDP-GlcA.

Table II. *Calibration of cell wall precursor analysis method using LC-MS/MS*

Retention time, linearity of the calibration, relative SD (RSD = 100 × SD/mean) of three concentration levels of standards, and limits of detection and quantification calculated for signal-to-noise ratio 3:1 and 10:1, respectively, were determined by the established LC-MS/MS method.

Metabolite	Retention Time	Linearity Range	Correlation Coefficient	Repeatability			Limit of Detection	Limit of Quantification
				100 pmol	1,000 pmol	2,000 pmol		
	min	*pmol*			*%RSD*		*pmol*	*pmol*
Gal1P	15.0	5–5,200	0.9920	3.96	2.27	3.53	1	4
Man1P + Glc1P	15.5	5–6,600	0.9968	5.06	1.77	3.08	0.8	3
Glc6P	25.3	5–5,500	0.9970	4.05	0.91	2.72	0.6	3
Fru6P	27.3	5–4,000	0.9963	3.41	2.41	4.49	2	5
Man6P	28.6	5–5,700	0.9955	4.59	0.46	3.80	2	6
ADP-Glc	31.6	25–4,000	0.9977	1.49	7.67	2.40	25	82
UDP-GalNAc	44.5	10–450	0.9748	7.27	8.48	2.16	2	5
UDP-GlcNAc	45.1	20–850	0.9870	5.30	8.15	1.08	5	16
UDP-Ara	46.6	5–900	0.9965	4.56	5.68	5.66	3	9
UDP-Gal	46.7	35–3,000	0.9956	5.11	7.77	2.52	34	111
UDP-Glc	48.4	25–3,400	0.9791	7.69	6.44	2.68	21	66
UDP-Xyl	49.2	2–750	0.9973	8.75	6.21	3.90	0.7	3
GDP-Fuc	52.4	4–1,600	0.9933	7.65	6.40	1.21	0.3	1
GDP-Man + GDP-Glc	54.2	35–14,300	0.9976	16.24	4.88	2.20	6	20
UDP-GalA	58.2	25–6,800	0.9938	9.31	11.93	2.17	12	38
UDP-GlcA	59.45	30–7,200	0.9940	1.62	11.22	2.65	27	88

activities in labeling. Metabolic flux analysis requires quantifying these compounds, their fractional and preferably also positional labeling, and the ability to analyze many time point samples. These requirements necessitated the development of a method that can be performed in medium to high throughput and achieves compound separation and quantitation, such as LC-MS/MS, and that also yields detailed labeling information.

In this study we have developed and validated a robust and sensitive LC-MS/MS method that successfully allows us to separate and quantify the levels and isotopic labeling of plant cell wall precursors. Using plant tissues from fenugreek (*Trigonella foenum-graecum*) endosperms and Arabidopsis (*Arabidopsis thaliana*) cell cultures, 12 hexose-Ps and NDP-sugars known to be involved in plant cell wall biosynthesis were separated and quantified. The direct analysis of intracellular cell

Table III. *Extraction efficiency and recovery of cell wall precursors from to Arabidopsis suspension cell*

Arabidopsis suspension cells were sampled and extracted as described in "Materials and Methods." Some samples were spiked with cell wall precursor standards before or after extraction. The average of normalized peak areas ± SD of three biological replicates are shown. The recovery was calculated as previously described by Cruz et al. (2008): Recovery = 100 [peak area (sample spiked before extraction) − peak area (sample)]/[peak area (sample spiked after extraction) − peak area (sample)]. nd, Not detected.

Metabolite	Arabidopsis Cell Extract (Normalized Peak Area)	Sample Spiked Before Extraction (Normalized Peak Area)	Sample Spiked After Extraction (Normalized Peak Area)	Recovery
				%
Gal1P	326 ± 24	925 ± 49	959 ± 128	95 ± 9
Man1P + Glc1P	2,142 ± 181	3,890 ± 183	3,683 ± 570	113 ± 10
Glc6P	12,321 ± 500	19,311 ± 2,527	18,443 ± 550	114 ± 7
Fru6P	8,315 ± 737	13,729 ± 1,863	14,223 ± 1,767	92 ± 12
Man6P	4,576 ± 208	7,027 ± 516	6,936 ± 564	104 ± 7
ADP-Glc	nd	967 ± 70	1,014 ± 57	95 ± 7
UDP-GalNAc	2,240 ± 63	22,644 ± 773	22,573 ± 2,032	100 ± 6
UDP-GlcNAc	5,780 ± 167	37,386 ± 1,719	36,373 ± 635	103 ± 3
UDP-Ara	255 ± 5	685 ± 19	706 ± 83	96 ± 6
UDP-Gal	1,080 ± 142	2,743 ± 46	2,794 ± 67	97 ± 4
UDP-Glc	11,445 ± 968	19,277 ± 261	18,281 ± 1,731	115 ± 6
UDP-Xyl	254 ± 14	1,879 ± 117	2,148 ± 185	86 ± 7
GDP-Fuc	604 ± 33	15,846 ± 472	17,554 ± 772	90 ± 4
GDP-Man + GDP-Glc	664 ± 70	18,961 ± 1,340	19,791 ± 256	96 ± 4
UDP-GalA	104 ± 7	1,299 ± 104	1,471 ± 16	87 ± 4
UDP-GlcA	288 ± 13	2,276 ± 175	2,437 ± 115	92 ± 6

wall precursors and their isotopic labeling significantly expands the set of tools for assessing the dynamics and regulation of cell wall biosynthesis, including the potential for dynamic metabolic flux analysis.

RESULTS AND DISCUSSION

Method Development: Cell Wall Precursor Separation and Identification

Figure 1 presents cell wall biosynthetic pathways (Seifert, 2004; Sharples and Fry, 2007; Reiter, 2008), involving six hexose-Ps: Glc-6-P (Glc6P), Glc-1-P (Glc1P), Fru-6-P (Fru6P), Gal-1-P (Gal1P), Man-1-P (Man1P), and Man-6-P (Man6P); and 11 NDP-sugars: UDP-Gal, UDP-Glc, UDP-Rha, UDP-GlcA, UDP-GalA, UDP-Xyl, UDP-apiose (UDP-Api), UDP-Ara, GDP-Man, GDP-Glc, and GDP-Fuc. Since all the precursors involved in cell biosynthesis are phosphorylated sugars, they are separable by liquid anion-exchange chromatography. This was implemented using an IonPac AS11 column (250 × 2 mm, Dionex) equipped with an AG11 guard column (50 × 2 mm, Dionex). To quantify the levels and the mass isotopomer distribution of hexose-Ps and NDP-sugars, we used a triple-quad Quattro Premier (Waters) operating in the negative ion mode. The combination of a specific retention time with a specific parent molecular ion, and a unique fragment (or daughter) ion, can be a sensitive method to unambiguously monitor and quantify metabolites of interest (van Dam et al., 2002; Huck et al., 2003; Grange et al., 2005; Bajad et al., 2006; Luo et al., 2007; Cruz et al., 2008; Arrivault et al., 2009). Since all cell wall precursors are phosphorylated, we optimized the collision parameters (Table I) for the formation of phosphate (m/z 79, 97) and diphosphate (m/z 159) ions. Each compound was thus followed at a specific parent/daughter transition. Since we were monitoring for different metabolites simultaneously, we used the multiple reaction monitoring (MRM) mode, which has the advantage of being highly selective and sensitive. Several gradients of sodium hydroxide (NaOH) concentration were tested to optimize the separation of cell wall precursors.

As shown in Figure 1, there are six hexose-Ps and 11 NDP-sugars involved in cell wall biosynthesis. In addition, other plant NDP-sugars, such as ADP-Glc, UDP-acetylglucosamine (GlcNAc), and UDP-acetylgalactosamine (GalNAc), have similar structure and masses and may affect the separation and detection of the ones participating in cell wall synthesis. The separation of cell wall precursors is shown in Figures 2 and 3. Separation was optimized using mixtures of the compounds listed above, with the exception of UDP-Rha and UDP-Api, which are not commercially available. For compound separation the gradient of eluent was started with 0.5 mM NaOH for 4 min and then it was linearly increased over 9 min to 4.1 mM NaOH. It was maintained at 4.1 mM NaOH for 7 min, which allows the elution of Gal1P, Man1P, and Glc1P. From 20 to 30 min, NaOH was increased from 4.1 to 10 mM in a linear fashion to elute Glc6P, Fru6P, and Man6P. Within the first 30 min of the run, this method successfully separates four hexose-Ps, with only one pair coeluting (Glc1P and Man1P; Fig. 2). NDP-sugars were eluted after 30 min with two consecutive linear gradients: the first one going from 10 to 20 mM NaOH in 15 min and then the second one from 20 to 50 mM NaOH in 15 min. Eleven NDP-sugars were separated by mass and/or retention time, only two of them coelute (GDP-Man and GDP-Glc; Fig. 3). After elution of cell wall precursors, the column was washed with 50 mM NaOH for 20 min. Because of the low purity and uncertain quantities of some standards we checked the quality and the real concentration of each standard by ^{1}H-NMR and ^{31}P-NMR (Supplemental Fig. S1; Supplemental Tables S1 and S2). Besides UDP-Gal and UDP-Glc there were two extra peaks at the transition 565/79 with the same retention time as UDP-GalNAc and UDP-GlcNAc. Those extra peaks correspond to UDP-GalNAc and UDP-GlcNAc that lost the acetyl group at the source.

Validation results for the established method are reported in Table II. In general, the calibration graphs showed excellent linearity over a wide range of concentrations (from low pmol to nmol levels) with correlation coefficients higher than 0.974. As shown in Table II, the limits of detection varied from 0.3 and 34 pmol and the limits of quantification were between

Table IV. *Quantification of cell wall precursors in Arabidopsis cells and fenugreek endosperms*

Arabidopsis T87 cell suspension culture and fenugreek endosperms were sampled as described in "Materials and Methods." Intracellular metabolites were extracted in boiling water, filtered, and concentrated before being analyzed by LC-MS/MS using the separation and hardware described in "Materials and Methods." The values reported below are the mean ± SD of three biological replicates and are expressed in pmol mg DW^{-1}. nd, Not detected.

Metabolite	Arabidopsis Cells	Fenugreek Endosperms
	pmol mg DW^{-1}	*pmol mg DW^{-1}*
Gal1P	123.6 ± 12.2	58.0 ± 10.1
Man1P + Glc1P	301.9 ± 14.1	50.9 ± 5.5
Glc6P	6,689.1 ± 434.4	864.4 ± 106.9
Fru6P	1,876.0 ± 135.4	296.8 ± 21.5
Man6P	733.2 ± 30.4	284.2 ± 42.6
ADP-Glc	nd	nd
UDP-GalNAc	22.4 ± 0.8	3.5 ± 0.4
UDP-GlcNAc	78.8 ± 2.4	14.3 ± 1.0
UDP-Ara	77.6 ± 9.7	24.9 ± 4.3
UDP-Gal	341.6 ± 4.6	63.1 ± 11.8
UDP-Glc	1,161.3 ± 161.2	98.6 ± 21.7
UDP-Xyl	7.5 ± 1.0	1.2 ± 0.2
GDP-Fuc	1.3 ± 0.3	0.3 ± 0.1
GDP-Man + GDP-Glc	42.3 ± 6.3	41.9 ± 10.3
UDP-GalA	23.1 ± 5.9	5.9 ± 1.7
UDP-GlcA	75.2 ± 14.8	8.7 ± 1.8

1 and 111 pmol. The limits of detection for the hexose-Ps were mostly below 2 pmol, whereas it was above 2 pmol for NDP-sugars. To check the method's repeatability, three concentration levels of standard mixture were injected three times and the SDS were less than 16%, 11.2%, and 5.7% for 100 pmol, 1,000 pmol, and 2,000 pmol of standard mixtures, respectively.

Application to Plant Extracts: Hexose-P and NDP-Sugar Profiling in Two Plant Tissues with Different Cell Wall Composition

We next applied the LC-MS/MS methodology to quantifying the cell wall precursors in different plant tissues. Live cells equivalent to approximately 10 mg dry weight (DW) of fenugreek endosperms and Arabidopsis T87 cell suspension cultures were frozen in liquid nitrogen. The extraction of cell wall precursors was performed with boiling water. Since plants contain high activities of nonspecific phosphatases (Duff et al., 1994), we checked the extraction efficiency and the recovery of cell wall precursors from Arabidopsis suspension cells by spiking samples with standards before or after extraction (Table III). Recoveries were above 87% whether standards were added before or after extraction. By contrast with studies of yeast or bacteria (Canelas et al., 2009), no quantitative evaluation of intracellular metabolite extraction techniques in plant tissues appears to have been published. When tested on *E. coli* and *Saccharomyces cerevisiae* and compared to other extraction methods (boiling ethanol, perchloric acid, or potassium hydroxide), the recoveries of intracellular metabolites after hot water extraction were excellent (Hans et al., 2001). Indeed, hot water was shown to extract efficiently phosphorylated metabolites such as nucleotides (Lundin and Thore, 1975) and intermediaries of glycolysis (Hiller et al., 2007). The recoveries that we obtained after hot water extraction were similar to those obtained by extraction with aqueous formic acid saturated with *n*-butanol on tobacco (*Nicotiana tabacum*) suspension cell cultures and cultured pollen tubes (Schlüpmann et al., 1994) and ice-cold methanol/chloroform (3:7, v/v) performed on Arabidopsis rosettes (Arrivault et al., 2009), and twice as high as the methanol/chloroform/formic acid/water (12:5:1:2, v/v/v/v) carried out on tobacco leaves (Cruz et al., 2008).

The LC-MS/MS analyses of hexose-Ps required 2% and NDP-sugars 20% of the total extract from both fenugreek endosperms and Arabidopsis cells (Supplemental Fig. S2 for Arabidopsis cells). Cell wall biosynthesis in fenugreek endosperms is of interest since this tissue accumulates up to 90% of galactomannan in their secondary cell wall (Edwards et al., 1992). The absolute quantities of hexose-Ps and NDP-sugars per mg DW are given in Table IV. The levels of cell wall precursors in Arabidopsis cells were up to 6 to 7 times higher than in fenugreek endosperms. However, for

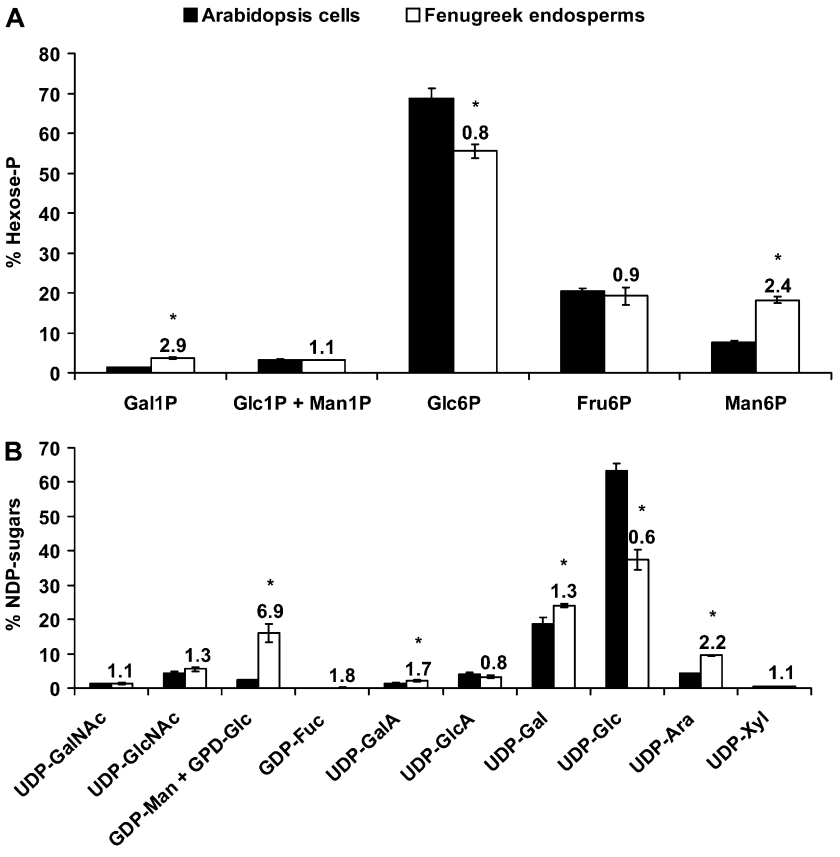

Figure 4. Cell wall precursor composition in Arabidopsis cells and fenugreek endosperms. Arabidopsis T87 cell suspension culture and fenugreek endosperms were sampled as described in "Materials and Methods." Intracellular metabolites were extracted in boiling water, filtered, and concentrated before being analyzed by LC-MS/MS using the separation and hardware described in "Materials and Methods." A and B, Hexose-P composition (A) and NDP-sugar composition (B) in Arabidopsis T87 cells in culture (black bars, mean ± SD, $n = 3$ biological replicates) and fenugreek endosperms 25 d after flowering (white bars, mean ± SD, $n = 3$ biological replicates). For each compound the asterisk (*) means that there is a significant difference at the $P < 0.05$ level (Tukey's studentized range test) between Arabidopsis cells and fenugreek endosperms.

both tissues, Glc6P and UDP-Glc were the main hexose-P and NDP-sugar, respectively. We were able to monitor several peaks for UDP-Rha in plant tissues (Supplemental Fig. S2) but since there is no UDP-Rha standard commercially available we could not identify it. In comparison to Arabidopsis cell cultures, the composition of hexose-Ps and NDP-sugars was significantly different in fenugreek endosperms (Fig. 4, A and B) with the percentages of Gal1P and Man6P being 2.9 and 2.4 times higher, respectively, in fenugreek endosperms than in Arabidopsis cell cultures. The proportion of Glc6P was significantly lower in fenugreek endosperm while the proportion of Glc1P + Man1P and Fru6P were not significantly different between the two plant tissues (Fig. 4A). Concerning the NDP-sugars, the percentages of GDP-Man + GDP-Glc, UDP-GalA, UDP-Gal, and UDP-Ara were significantly higher in fenugreek endosperms—by factors of, respectively, 6.9, 1.7, 1.3, and 2.2. The percentage UDP-Glc was 0.6 times lower in fenugreek endosperm in comparison to Arabidopsis cells (Fig. 4B). These results show that the proportions of the precursors of galactomannan, which accounts for 90% of the secondary cell wall in fenugreek endosperms, are much higher than in undifferentiated heterotrophic cells.

Application to ^{13}C-Labeled Plant Extracts

Arabidopsis T87 cells were incubated with 100% [U-$^{13}C_{Fru}$]Suc until isotopic steady state was reached. When ^{13}C-labeled substrates are supplied, steady-state labeling of the metabolites reflects the relative fluxes through different metabolic pathways (Libourel and Shachar-Hill, 2008). After labeling, phosphorylated

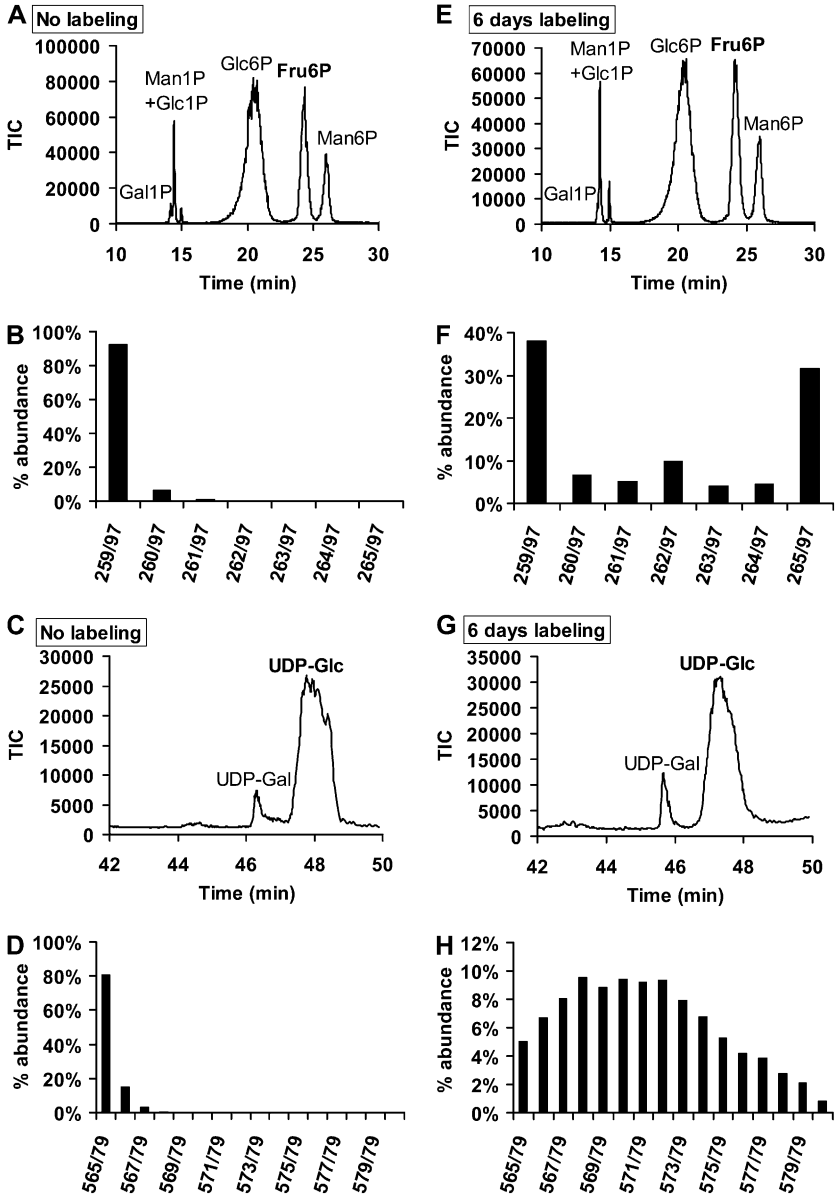

Figure 5. MRM application to steady-state ^{13}C-labeling analysis of Fru6P and UDP-Glc. Arabidopsis cells were grown in medium containing 100% [U-$^{13}C_{Fru}$]Suc until isotopic steady state was reached. Phosphorylated metabolites were extracted as previously described and analyzed by LC-MS/MS. The selected daughter ions are $[H_2PO_4]^-$ (m/z = 97) for Fru6P and $[PO_3]^-$ (m/z = 79) for UDP-Glc. For a phosphorylated metabolite containing n atoms of carbon, we follow n + 1 transitions: $[M_0\text{-H}]^-/97$, $[M_{+1}\text{-H}]^-/97 \ldots [M_{+n}\text{-H}]^-/97$. A, TIC of the transitions 259/97 through 265/97 before labeling. B, Mass isotopomer distribution of Fru6P before labeling. C, TIC of the transitions 565/79 through 580/79 before labeling. D, Mass isotopomer distribution of UDP-Glc before labeling. E, TIC of the transitions 259/97 through 265/97 after 6 d of labeling. F, Mass isotopomer distribution of Fru6P after 6 d of labeling. G, TIC of the transitions 565/79 through 580/79 after 6 d of labeling. H, Mass isotopomer distribution of UDP-Glc after 6 d of labeling.

metabolites were extracted and analyzed by LC-MS/MS. The selected daughter ions were $[PO_3]^-$ (m/z = 79), $[H_2PO_4]^-$ (m/z = 97), and $[HP_2O_6]^-$ (m/z = 159; Table I). We applied the MRM mode to quantifying ^{13}C labeling in hexose-Ps and NDP-sugars using MS/MS fragment ions that contain no carbon for detection (Fig. 5). For a phosphorylated metabolite containing n carbon atoms, we follow $n + 1$ transitions: $[M_0\text{-}H]^-/97$, $[M_{+1}\text{-}H]^-/97$…$[M_{+n}\text{-}H]^-/97$. The carbon labeling of the molecule ion can then be obtained directly from the intensity of selected MS/MS transitions where the observed fragment is a phosphate group (Kiefer et al., 2007). The total ion count (TIC) of the transitions 259.1/97.0, 260.1/97.0…265.1/97.0 corresponding to the hexose-Ps were monitored in an unlabeled culture (Fig. 5A), and the mass isotopomer distribution of the Fru6P showed natural abundance labeling (Fig. 5B). For UDP-Glc and UDP-Gal, we followed the transitions 565.0/79.0 through 580.0/79.0 in an unlabeled culture (Fig. 5C), and the mass spectra for the UDP-Glc reflected natural abundance distribution (Fig. 5D). After labeling to steady state the extracts from Arabidopsis T87 cells revealed TICs for hexose-Ps (Fig. 5E) and UDP-Gal/UDP-Glc (Fig. 5G) similar to unlabeled cultures (Fig. 5, A and C). However, after labeling with 100% [U-$^{13}C_{Fru}$]Suc, the mass isotopomer spectra of Fru6P (Fig. 5F) and UDP-Glc (Fig. 5H) were very different from the ones of the unlabeled culture (Fig. 5, A and D, respectively). The mass abundance distribution for Fru6P, as an example, showed a decrease of M_0 (259/97) ions and increases in the percentage of labeled molecules, mostly M_{+6} (265/97) and M_{+3} (262/97; Fig. 5F). Only 5.1% of the UDP-Glc remained fully unlabeled whereas the abundances of different labeled UDP-Glc forms (isotopomers) contained between 0.8% and 9.6% of TIC, reflecting a high degree of rearrangement of label within this molecule (Fig. 5H). It is important to note that only the sugar component of the NDP-sugar is incorporated into cell wall. One way to access the labeling of this sugar component is to measure the labeling in the free nucleotide and then to substract it from the complete NDP-sugar, thus leaving only the mass spectrum of the sugar component (Supplemental Fig. S3).

This labeling information is very valuable for identifying the pathways involved in carbon rearrangements and quantifying the fluxes through them (Ratcliffe and Shachar-Hill, 2006). For instance, the increase in the M_{+6} isotopomer of Fru6P reflects Suc degradation into Fru and Glc and then the direct phosphorylation of Fru into Fru6P. The fact that the M_{+6} abundance of Fru6P went from 0% (Fig. 5B) to 31.6% (Fig. 5F) after labeling with [U-$^{13}C_{Fru}$]Suc showed that there was a rapid exchange between the Glc6P and Fru6P that causes dilution of the label that enters directly into the Fru6P pool by unlabeled Glc6P via isomerization by hexose-P isomerase. The increase of the M_{+3} of Fru6P from 0% (Fig. 5B) to 9.9% (Fig. 5F) revealed active hexose-P/triose-P cycling (Fig. 1).

We applied this method to follow the labeling of cell wall precursors during pulse labeling experiment with [U-$^{13}C_{Fru}$]Suc in Arabidopsis T87 suspension cells (Fig. 6). The abundance of unlabeled hexose-Ps (259/97) decreased as these pools became labeled and the rate of decrease for each one depended on the position of that hexose-P in the network (Fig. 1) and the amplitude of the fluxes between them. The levels of fully labeled molecules (265/97) increased at rates that reflect the same sequence. The direct analysis of labeling in

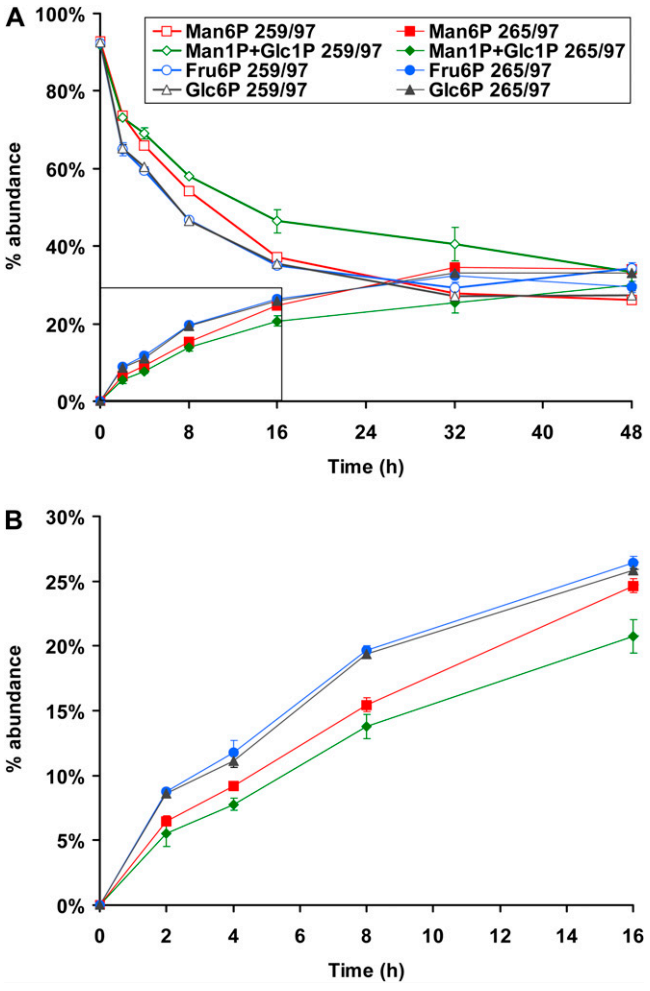

Figure 6. MRM application to pulse $^{-}$C-labeling analysis of hexose-Ps. Arabidopsis cells were labeled with 100% [U-$^{13}C_{Fru}$]Suc. For each time point, 3 mL of cell suspension culture were sampled by filtration, and the phosphorylated metabolites were extracted in boiling water and analyzed by LC-MS/MS as described in "Materials and Methods." The selected daughter ions are $[H_2PO_4]^-$ (m/z = 97) and we followed the transitions 259/97 through 265/97, corresponding to the hexose-Ps. Empty blue circles, black triangles, red squares, and green diamonds represent the relative abundance of unlabeled Fru6P, Glc6P, Man6P, and Man1P + Glc1P, respectively. The filled blue circles, black triangles, red squares, and green diamonds represent the relative abundance of fully labeled Fru6P, Glc6P, Man6P, and Man1P + Glc1P, respectively. Error bars represent SD of three biological replicates. B is a magnification of region framed in A.

intracellular cell wall precursors such as hexose-Ps and NDP-sugars illuminates the dynamics of this area of plant metabolism, allowing a deeper understanding of in vivo kinetics and metabolic activity regulation. Kinetic modeling of datasets such as these (Rios-Estepa and Lange, 2007; Libourel and Shachar-Hill, 2008) allows the construction and validation of mechanistic predictive models.

CONCLUSION

We have developed and validated a method that allows the separation, quantification, and labeling analysis of the large majority of plant cell wall precursors. The method uses anion-exchange-based LC/MS-MS operating in MRM mode and allows sensitive reproducible quantification over several orders of magnitude of concentration. With unlabeled plant extracts from Arabidopsis T87 cell suspension cultures and fenugreek endosperm, we determined the concentrations of cell call precursors in vivo with high recovery rates and assessed the quantity of plant material needed for the analyses of these compounds. Using ^{13}C-labeled Suc, steady-state and pulse-labeling experiments in Arabidopsis T87 cell suspension cultures showed that this method is suitable for analyzing metabolic flux through cell wall precursors, which are some of the largest fluxes of carbon in biology.

MATERIALS AND METHODS

Chemicals

UDP-Xyl, UDP-Ara, and UDP-GalA were purchased from the Complex Carbohydrate Research Center (University of Georgia). All the other NDP-sugars and hexose-Ps, with the exception of UDP-Api and UDP-Rha, which are not commercially available, were purchased from Sigma. We checked the purity and concentration of all the standards we used by ^{1}H-NMR and ^{31}P-NMR (Supplemental Fig. S1; Supplemental Tables S1 and S2). To avoid carbonate contamination, the NaOH was purchased from Fluka in liquid form. All the water used as eluent and reagent was deionized and degassed. [U-$^{13}C_{Fru}$]Suc was purchased from Omicron Biochemicals, Inc.

High-Performance Anion-Exchange Chromatography

The LC was performed with an ACQUITY UPLC pump system (Waters). The eluents were vacuum degassed. Samples in the autosampler were kept at 4°C, whereas the LC analysis was carried out at room temperature. Phosphorylated metabolites were separated by ion chromatography on an IonPac AS11 (250 × 2 mm, Dionex) column equipped with a guard column AG11 (50 × 2 mm, Dionex) at a flow rate of 0.35 mL min^{-1}. The NaOH gradient was generated from 0.5 mM NaOH (A) and 50 mM NaOH (B). The initial condition was 100.0% A (0.5 mM NaOH) for 2 min. The fraction of B was increased in a linear fashion to 7.3% (4.1 mM NaOH) in 11 min and maintained for 7 min. The fraction of B was linearly increased to 19.2% (10 mM NaOH) in 10 min, to 39.4% B (20 mM NaOH) in 15 min, and then to 100.0% B (50 mM NaOH) in 15 min. Cleaning the column is achieved by maintaining B at 100.0% (50 mM NaOH) for 20 min. The initial conditions were restored in 0.1 min, followed by 5 min of column equilibration.

NaOH Suppression

NaOH concentration of the eluent is too high for a proper mass spectrometric analysis and was reduced with a post-column anion self-regenerating suppressor ASRS 300 (2 mm, Dionex). It was operated in the AutoSuppression External Water Mode for high sensitivity analysis. The current applied on the ASRS was 50 mA and the reagent flow rate was 4 mL min^{-1}.

MS

The MS/MS analyses were performed with a Quattro-Premier (Waters), triple quadrupole mass spectrometer. Mass spectra were acquired using electrospray ionization in negative ion mode and MRM. The capillary voltage, extractor voltage, and rangefinder lens setting were set at 3.00 kV, 5 V, and 0.0, respectively. The flow rates of cone gas and desolvation gas were 50 and 800 L h^{-1}, respectively. The source temperature and desolvation temperature were 100°C and 350°C, respectively. The [M-H]$^{-1}$ were fragmented by collision-induced dissociation with argon as collision gas at a manifold pressure of 2.67×10^{-3} mbar. Collision energies and source cone potentials were optimized for each transition using Waters QuanOptimize software (Table I). Data were acquired with MassLynx 4.0 and processed for calibration and for quantification of the analytes with QuanLynx software.

Arabidopsis Cell Cultures

Arabidopsis (*Arabidopsis thaliana*) ecotype Columbia suspension-cultured cells (Jouanneau and Péaud-Lenoël, 1967) were obtained from the Riken BioResource Center (hppt://www.brc.riken.jp). T87 cells were maintained in a 7 d culture interval under continuous dark at 22°C with shaking at 120 rpm in a media containing: 4.3g L^{-1} Murashige and Skoog basal salt mixture, 0.2 mg L^{-1} thiamine, 20 mg L^{-1} myoinositol, 3 mL L^{-1} Miller's I, 0.2 mL L^{-1} 2,4-dichlorophenoxyacetic acid, 30 g L^{-1} Suc, and pH adjusted to 5.8. Culture growth was followed by measuring the A_{600} ($OD_{600\ nm}$) ranging from 0.1 and 0.5. For the sampling, between 1 and 3 mL of suspension culture (approximately $OD_{600\ nm}$ = 3) was quickly filtered through a nylon membrane filter (Whatman; 0.45 μm pore size and 47 mm diameter). The filter containing the cells was then transferred into a falcon tube before being placed into liquid nitrogen. The overall process took less than 20 s.

Fenugreek Endosperms

Fenugreek (*Trigonella foenum-graecum*) plants were grown based on the approach published by Edwards et al. (1989) with modifications. Fenugreek seeds were purchased from BulkFoods.com. The seeds were germinated on wet paper towel in a 150-mm petri dish at room temperature in dark for 2 d, and the germinated seedlings were then transferred to pots containing BACCTO professional planting mix (Michigan Peat Company) with one-quarter sand. The fenugreek seedlings were grown in the light cycle of 12 h light at 22°C and 12 h dark at 20°C with photon fluence rate of 200 μmol m^{-2}. Secondary inflorescence stems were trimmed away regularly. Nutrient solution prepared by dissolving 0.5 g of Peters professional water-soluble fertilizer (General Purpose 20-20-20, The Scotts Company) in 1 L of water was applied weekly only after plants start flowering (about 6 weeks after germination). Flowers were tagged at anthesis. Approximately 10 fenugreek endosperms 25 d after flowering were dissected out from seeds and frozen immediately in liquid nitrogen. The frozen endosperms were stored at −80°C before use.

Extraction of Intracellular Metabolites

Intracellular metabolites were extracted using boiling water. This procedure was adapted from Martínez-Force and Benítez (1995). Three milliliters of boiling water was added to frozen tubes containing Arabidopsis T87 cells or fenugreek endosperms. Tubes were quickly immersed in a water bath at 95°C to 100°C for 10 min and vortexed once after five min. Each tube was then placed on ice, and the extracts were filtered through 0.22-μm pore syringe filters. The samples and syringe filters were rinsed twice with 1 mL of water. The extract were then stored at −20°C until further use. After thawing, hot water extracts were evaporated under vacuum at 50°C using a CentriVac concentrator (Labconco). Dried residues of Arabidopsis cells and fenugreek endosperms were resuspended in 50 or 100 μL of Milli-Q water, respectively, to be analyzed by LC-MS/MS.

Supplemental Data

The following materials are available in the online version of this article.

Supplemental Figure S1. NMR spectra of cell wall standards.

Supplemental Figure S2. LC-MS/MS analyses of Arabidopsis cell extracts.

Supplemental Figure S3. Extraction of the mass spectrum of Glc from UDP-Glc.

Supplemental Table S1. Chemical shifts of cell wall standards.

Supplemental Table S2. Real concentration of standards of cell wall precursors.

ACKNOWLEDGMENTS

We are grateful to Professor Dan Jones and Lijun Chen of the Michigan State University MS facility for helpful advice and access to the LC-MS/MS equipment. We thank Daniel Holmes of the Michigan State University NMR facility, David Cavalier for help with Dionex equipment, and Linda Danhof for help with Arabidopsis T87 cells cultures.

Received March 2, 2010; accepted May 3, 2010; published May 4, 2010.

LITERATURE CITED

Allwood JW, Goodacre R (2010) An introduction to liquid chromatography-mass spectrometry instrumentation applied in plant metabolomic analyses. Phytochem Anal **21:** 33–47

Arrivault S, Guenther M, Ivakov A, Feil R, Vosloh D, van Dongen JT, Sulpice R, Stitt M (2009) Use of reverse-phase liquid chromatography, linked to tandem mass spectrometry, to profile the Calvin cycle and other metabolic intermediates in Arabidopsis rosettes at different carbon dioxide concentrations. Plant J **59:** 824–839

Bajad SU, Lu W, Kimball EH, Yuan J, Peterson C, Rabinowitz JD (2006) Separation and quantification of water soluble cellular metabolites by hydrophilic interaction chromatography-tandem mass spectrometry. J Chromatogr A **1125:** 76–88

Canelas AB, ten Pierick A, Ras C, Seifar RM, van Dam JC, van Gulik WM, Heijnen JJ (2009) Quantitative evaluation of intracellular metabolite extraction techniques for yeast metabolomics. Anal Chem **81:** 7379–7389

Cruz JA, Emery C, Wüst M, Kramer DM, Lange BM (2008) Metabolite profiling of Calvin cycle intermediates by HPLC-MS using mixed-mode stationary phases. Plant J **55:** 1047–1060

Duff SMG, Sarath G, Plaxton WC (1994) The role of acid-phosphates in plant phosphorus-metabolism. Physiol Plant **90:** 791–800

Edwards M, Bulpin PV, Dea ICM, Reid JSG (1989) Biosynthesis of legume-seed galactomannan in vitro. Planta **178:** 41–51

Edwards M, Scott C, Gidley MJ, Reid JSG (1992) Control of mannose galactose ratio during galactomannan formation in developing legume seeds. Planta **187:** 67–74

Feingold DS, Barber GA (1990) Nucleotide sugars. *In* PM Dey, JB Harborne, eds, Methods in Plant Biochemistry, Vol 2. Academic Press, London, pp 39–78

Fry SC (2000) The Growing Plant Cell Wall: Chemical and Metabolic Analysis, Reprint Edition. Blackburn Press, Caldwell, NJ

Fry SC (2004) Primary cell wall metabolism: tracking the careers of wall polymers in living plant cells. New Phytol **161:** 641–675

Grange AH, Winnik W, Ferguson PL, Sovocool GW (2005) Using a triple-quadrupole mass spectrometer in accurate mass mode and an ion correlation program to identify compounds. Rapid Commun Mass Spectrom **19:** 2699–2715

Hans MA, Heinzle E, Wittmann C (2001) Quantification of intracellular amino acids in batch cultures of *Saccharomyces cerevisiae*. Appl Microbiol Biotechnol **56:** 776–779

Hiller J, Franco-Lara E, Weuster-Botz D (2007) Metabolic profiling of *Escherichia coli* cultivations: evaluation of extraction and metabolite analysis procedures. Biotechnol Lett **29:** 1169–1178

Huck JHJ, Struys EA, Verhoeven NM, Jakobs C, van der Knaap MS (2003) Profiling of pentose phosphate pathway intermediates in blood spots by tandem mass spectrometry: application to transaldolase deficiency. Clin Chem **49:** 1375–1380

Jouanneau JP, Péaud-Lenoël C (1967) Growth and synthesis of proteins in cell suspensions of a kinetin dependent tobacco. Physiol Plant **20:** 834–850

Kiefer P, Nicolas C, Letisse F, Portais JC (2007) Determination of carbon labeling distribution of intracellular metabolites from single fragment ions by ion chromatography tandem mass spectrometry. Anal Biochem **360:** 182–188

Libourel IGL, Shachar-Hill Y (2008) Metabolic flux analysis in plant: from intelligent design to rational engineering. Annu Rev Plant Biol **59:** 625–650

Lundin A, Thore A (1975) Comparison of methods for extraction of bacterial adenine-nucleotides determined by firefly assay. Appl Microbiol **30:** 713–721

Luo B, Groenke K, Takors R, Wandrey C, Oldiges M (2007) Simultaneous determination of multiple intracellular metabolites in glycolysis, pentose phosphate pathway in tricarboxylic acid cycle by liquid chromatography-mass spectrometry. J Chromatogr A **1147:** 153–164

Martínez-Force E, Benítez T (1995) Effects of varying media, temperature, and growth rates on the intracellular concentrations of yeast amino acids. Biotechnol Prog **11:** 386–392

Pauly M, Keegstra K (2008a) Cell-wall carbohydrates and their modification as a resource for biofuels. Plant J **54:** 559–568

Pauly M, Keegstra K (2008b) Physiology and metabolism 'Tear down this wall'. Curr Opin Plant Biol **11:** 233–235

Räbinä J, Mäki M, Savilahti EM, Järvinen N, Penttilä L, Renkonen R (2001) Analysis of nucleotide sugars from cell lysates by ion-pair solid-phase extraction and reversed-phase high-performance liquid chromatography. Glycoconj J **18:** 799–805

Ratcliffe RG, Shachar-Hill Y (2006) Measuring multiple fluxes through plant metabolic networks. Plant J **45:** 490–511

Reiter WD (2008) Biochemical genetics of nucleotide sugar interconversion reactions. Curr Opin Plant Biol **11:** 236–243

Rios-Estepa R, Lange BM (2007) Experimental and mathematical approaches to modeling plant metabolic networks. Phytochemistry **68:** 2351–2374

Schlüpmann H, Bacic A, Read SV (1994) Uridine diphosphate glucose metabolism and callose synthesis in culture pollen tubes of *Nicotiana alata* Link et Otto. Plant Physiol **105:** 659–670

Seifert GJ (2004) Nucleotide sugar interconversions and cell wall biosynthesis: how to bring the inside to the outside. Curr Opin Plant Biol **7:** 277–284

Sharples SC, Fry SC (2007) Radioisotope ratios discriminate between competing pathways of cell wall polysaccharide and RNA biosynthesis in living plant cells. Plant J **52:** 252–262

Somerville C, Bauer S, Brininstool G, Facette M, Hamann T, Milne J, Osborne E, Paredez A, Persson S, Raab T, et al (2004) Towards a systems approach to understanding plant-cell walls. Science **306:** 2206–2211

Turnock DC, Ferguson MAJ (2007) Sugar nucleotide pools of *Trypanosoma brucei*, *Trypanosoma cruzi*, and *Leishmania major*. Eukaryot Cell **6:** 1450–1463

van Dam JC, Eman MR, Frank J, Lange HC, van Dedem GWK, Heijnen SJ (2002) Analysis of glycolytic intermediates in *Saccharomyces cerevisiae* using anion exchange chromatography and electrospray ionization with tandem mass spectrometric detection. Anal Chim Acta **460:** 209–218

Wolfender JL, Glauser G, Boccard J, Rudaz S (2009) MS-based plant metabolomic approaches for biomarker discovery. Nat Prod Commun **4:** 1417–1430